Synthetic Metals 161 (2011) 1330–1335

Contents lists available at ScienceDirect

Synthetic Metals

journal homepage: www.elsevier.com/locate/synmet

Synthesis and characterization of a novel fullerene derivative containing carbazole group for use in organic solar cells

Dongbo Mi[a], Ji-Hoon Kim[a], Sung Cheol Yoon[b], Changjin Lee[b], Jin-Kyun Lee[c], Do-Hoon Hwang[a,*]

[a] Department of Chemistry, and Chemistry Institute for Functional Materials, Pusan National University, Busan 609-735, Republic of Korea
[b] Korea Research Institute of Chemistry Technology, 100 Jang-dong, Yuseong-gu, Daejeon 305-343, Republic of Korea
[c] Department of Polymer Science and Engineering, Inha University, Incheon 402-751, Republic of Korea

ARTICLE INFO

Article history:
Received 15 January 2011
Received in revised form 21 April 2011
Accepted 28 April 2011
Available online 25 May 2011

Keywords:
Fullerene derivatives
Carbazole
Organic solar cell

ABSTRACT

A novel carbazole-group-containing fullerene derivative (CBZ-C_{60}) with good solubility in common organic solvents was synthesized. This derivative was analyzed by using many techniques such as NMR, FAB-MS, FTIR and UV–vis absorption spectroscopy. Further, bulk heterojunction photovoltaic devices were fabricated. Since the LUMO energy level of CBZ-C_{60} was higher than that of fullerene, the open-circuit voltage (V_{oc}) of devices based on CBZ-C_{60} was higher than that of devices based on fullerene. The power-conversion efficiency was highest for devices with composite thin films that have P3HT/CBZ-C_{60} composition ratios of 1:1 and were annealed at 150 °C for 10 min. The maximum V_{oc}, short-circuit current density, and PCE of the best device were 0.64 V, 2.32 mA/cm^2, and 0.48%, respectively.

1. Introduction

Organic solar cells composed of organic electron donor and acceptor composites have been attracting considerable interest as a potential source of renewable energy because they are cost-effective and flexible [1–3]. Many types of low-band-gap conjugated polymers that act as p-type electron donors have been synthesized for use in organic photovoltaic (OPV) devices. However, only a few n-type electron acceptors have been reported for use in OPV devices. Fullerene (C_{60}) has been known to act as an efficient electron acceptor in OPV devices because of its high electron mobility. C_{60} films are usually prepared by evaporation because the solubility of C_{60} in common organic solvents is low. C_{60} is not suitable for preparing composite layers, especially when a bicontinuous-network morphology is desired, because of its strong tendency to crystallize. C_{60} derivatives that exhibit high solubility in common organic solvents and whose solutions do not show phase separation have been developed for use in heterojunction organic solar cells. During the last decade, [6,6]-phenyl-C61-butyric acid methyl ester (PCBM), a soluble C_{60} derivative, has been widely used to fabricate bulk heterojunction (BHJ) OPV devices [4–6]. By controlling the HOMO and LUMO energy levels of soluble C_{60} derivatives, the performance of photovoltaic devices could be improved. In this study, we synthesized new C_{60} derivatives with an N-ethylhexylcarbazole moiety via a carbene addition intermediate [7]. It has been reported that an increase in the LUMO energy level of the electron acceptor could result in an increase in the open-circuit voltage (V_{oc}), which in turn would lead to an improvement in the power-conversion efficiency [8]. We expected that the electron-rich carbazole group would increase the LUMO energy level of C_{60} even though it is not directly conjugated with C_{60}. The chemical structure and synthetic route to the novel C_{60} derivative are shown in Scheme 1.

2. Experiment

2.1. Measurements and device fabrication

The ^{1}H NMR and ^{13}C NMR spectrum was recorded using a Bruker AM-400 spectrometer; the absorption spectra, by using a Hitachi spectrophotometer model U-3501; and the Fourier-transform infrared (FTIR) spectra, by using a JASCO FTIR 460 plus spectrometer. EM (EI) was measured by using 7890A-5975C GC/MSD and FAB-MS was measured by using JEOLJMS-DX-303 Mass spectrometer. The cyclic-voltametry (BAS 100) was performed with a solution of tetrabutylammonium tetrafluoroborate (Bu_4NBF_4) (0.10 M) as the electrolyte and material (10^{-3} M) in 1,2-dichlorobenzenen at a scan rate of 50 mV/s at room temperature under argon atmosphere. A glassy carbon electrode (0.3 mm diameter) was used as the working electrode. A Pt and an Ag/AgCl electrode were used as the counter electrode and reference electrode. Composite solutions of P3HT and the synthesized C_{60} derivative were prepared using chlorobenzene as the solvent. The concentration of the composite solution was maintained in the range of 1.0–2.0 wt%.

* Corresponding author. Tel.: +82 51 510 3893; fax: +82 51 516 7421.
E-mail address: dohoonhwang@pusan.ac.kr (D.-H. Hwang).

0379-6779/$ – see front matter © 2011 Elsevier B.V. All rights reserved.
doi:10.1016/j.synthmet.2011.04.031

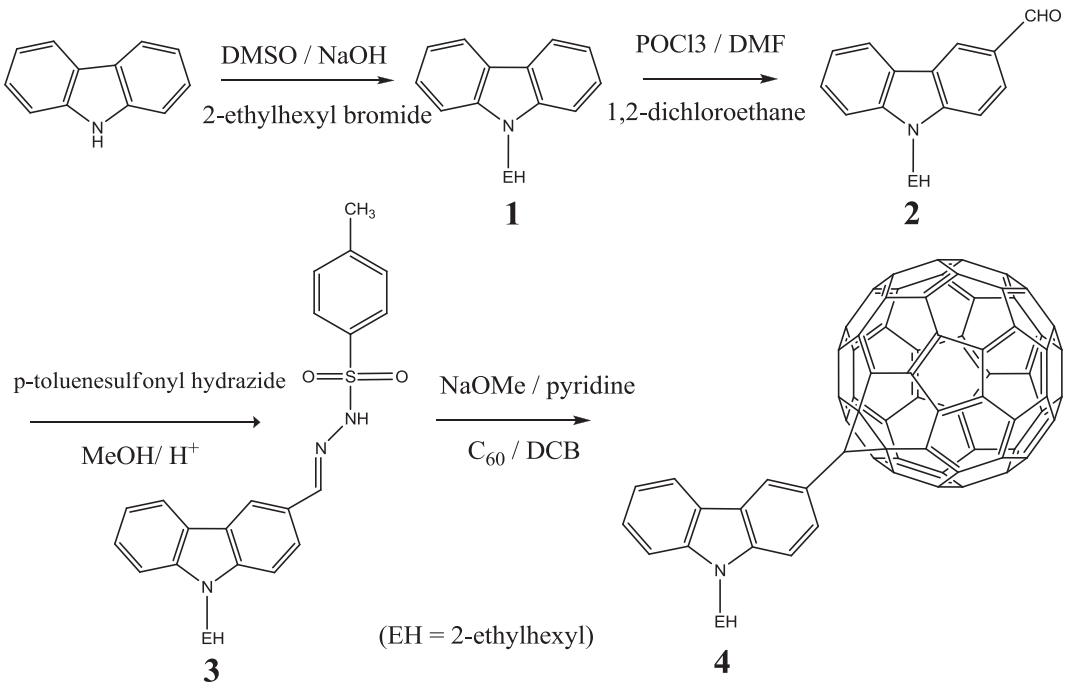

Scheme 1. Synthetic route for the carbazole-group containing fullerene derivative (CBZ-C_{60}).

Polymer photovoltaic devices with a typical sandwich structure of ITO/PEDOT:PSS/active layer/LiF/Al were fabricated. The ITO-coated glass substrates were cleaned by a routine cleaning procedure that involved sonication in a detergent followed by sonication in distilled water, in acetone, and finally, in 2-propanol. A 45-nm-thick layer of PEDOT:PSS (Baytron P) was spin coated on a cleaned ITO substrate after exposing the ITO surface to ozone for 10 min. The PEDOT:PSS layer was dried on a hot plate at 140 °C for 10 min. The pre-dissolved composite solution was filtered through 0.45 μm syringe filters and an active layer was spin coated over the PEDOT:PSS layer. Finally, a compound cathode (top electrode) consisting of a 0.5-nm thick layer of LiF and a 120-nm thick layer of Al were deposited onto the active polymer layer under vacuum of 3×10^{-6} torr in a thermal evaporator. The current–voltage (*I–V*) characteristics of all the polymer photovoltaic cells were measured under the simulated solar light (100 mW/cm^2; AM 1.5 G) provided by an Oriel 1000 W solar simulator. Electric data were recorded using a Keithley 236 source-measure unit, and characterizations were carried out in an ambient environment. The intensity of the simulated solar light was calibrated by a standard Si photodiode detector (PV measurements Inc.), which was calibrated at

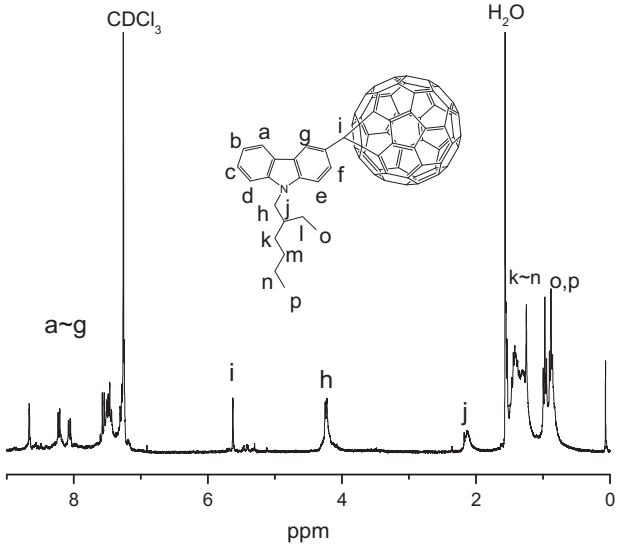

Fig. 1. ^{1}H NMR spectrum for CBZ-C_{60} ($CDCl_3$, 400 MHz).

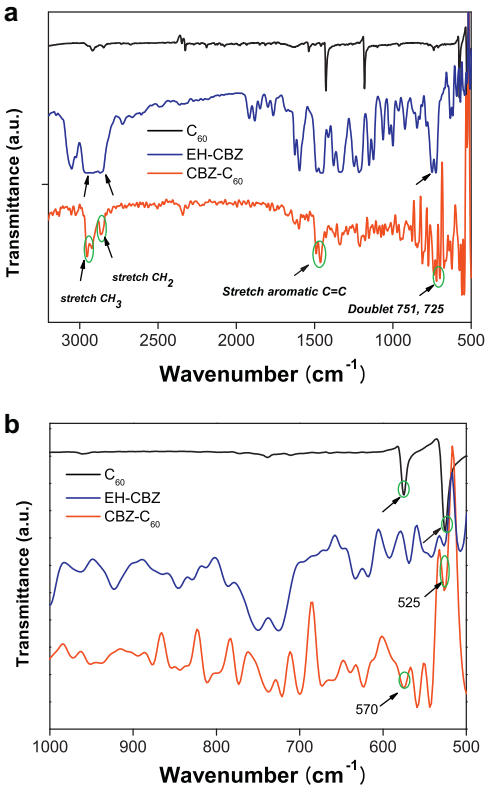

Fig. 2. (a) FTIR spectra of C_{60}, 9-(2-ethylhexyl)-9H-carbazole, and CBZ-C_{60}. (b) FTIR spectra of C_{60}, 9-(2-ethylhexyl)-9H-carbazole, and CBZ-C_{60} in fingerprint region.

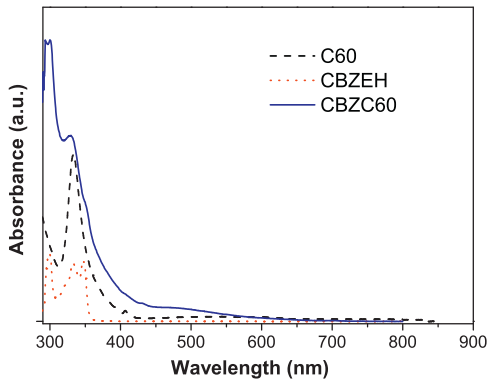

Fig. 3. UV–vis absorption spectra of C_{60}, 9-(2-ethylhexyl)-9H-carbazole, and CBZ-C_{60} in chlorobenzene.

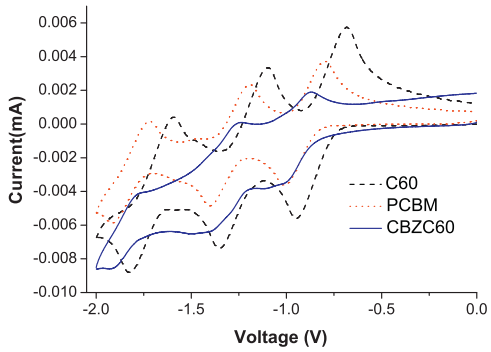

Fig. 4. Cyclic voltammograms of C_{60}, PCBM and CBZ-C_{60}.

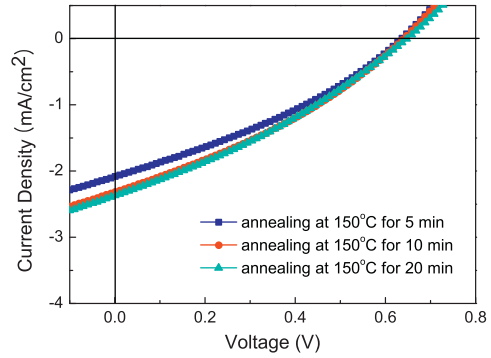

Fig. 5. Current–voltage (I–V) curves of the device with P3HT/CBZ-C_{60} (composition ratio = 1:1)

NREL. The thickness of the thin film was measured using a KLA Tencor Alpha-step IQ surface profilometer with an accuracy of ±1 nm.

2.2. Synthesis of CBZ-C_{60}

*9-(2-Ethylhexyl)-9H-carbazole (**1**).* Carbazole (20.0 g, 0.12 mol) and sodium hydroxide (28.8 g, 0.72 mol) were dissolved in 200 mL of DMSO, and the reaction mixture was stirred for 30 min at room temperature. 2-Ethylhexylbromide (27.7 mL, 0.156 mol) was added to the reaction mixture, and the resulting mixture was stirred for 24 h at room temperature. The reaction mixture was extracted three times using dichloromethane and brine. The organic layer was separated and dried with anhydrous magnesium sulfate, and then, the solvent was removed by using a rotary evaporator. The crude product (**1**) was purified by column chromatography using hexane/dichloromethane (composition ratio = 9:1) as the eluent. The product yield was 85.3% (28.6 g). ^{1}H NMR (400 MHz, $CDCl_3$): δ (ppm) 8.10 (d, 2H), 7.47–7.38 (m, 4H), 7.22–7.20 (m, 2H), 4.16 (q, 2H), 2.1 (m, 1 H), 1.40–1.25 (m, 8H), 0.89 (t, 3H), 0.86 (t, 3H). ^{13}C NMR (400 MHz, $CDCl_3$): δ (ppm) 141.03, 125.67, 122.93, 120.411, 118.83, 109.09, 47.33, 39.48, 31.09, 28.94, 24.50, 23.24, 14.25, 11.04. EM (EI) (M^+, $C_{20}H_{25}N$): calcd, 279.2; found, 279.2.

Table 1
Characteristics of BHJ solar cells with P3HT/CBZ-C_{60} (composition ratio = 1:1) thin films annealed for different durations.

	Annealing time (min)		
	5	10	20
V_{oc} (V)	0.64	0.64	0.65
J_{sc} (mA/cm^2)	2.08	2.32	2.37
FF (%)	32.7	32.6	31.1
PCE (%)	0.43	0.48	0.48

*9-(2-Ethylhexyl)-9H-carbazole-3-carbaldehyde (**2**).* Compound 2 was synthesized from 1 by Vilsmeier formylation. A 250 mL two-necked flask containing 50 mL anhydrous 1,2-dichloroethane was cooled in an ice bath. To the 1,2-dichloroethane solution, 2.83 mL (35.78 mmol) of anhydrous DMF was added and the resulting solution was cooled in an ice bath. To this solution, 2.1 mL (23.26 mmol) of phosphorus chloride was added in a dropwise manner for 30 min. Then, 5 g of 1 (17.89 mmol) in 10 mL of anhydrous 1,2-dichloroethane was added to the above mentioned solution in a dropwise manner for 30 min. Next, the ice bath was removed and the solution was heated to room temperature and then to 90 °C for 24 h. This solution was cooled to room temperature, and then poured into ice water; the solution thus obtained was neutralized by adding sodium acetate solution to it. The reaction mixture was extracted using dichloromethane and brine. The organic layer was dried with anhydrous magnesium sulfate and then concentrated in a rotary evaporator. The crude product was purified by column chromatography using ethyl acetate (EA)/hexane (composition ratio = 1:4) as the eluent. The yield of the product 2, a yellow solid, was 77.3% (4.25 g). ^{1}H NMR (400 MHz, $CDCl_3$): δ (ppm) 10.08 (s, 1H), 8.60 (s, 1H), 8.14 (d, 1H), 7.98 (d, 1H), 7.51–7.44 (m, 3H), 7.30 (m, 1H), 4.19 (m, 2H), 2.05 (m, 1H), 1.38–1.29 (m, 8H), 0.89 (t, 3H), 0.86 (t, 3H). ^{13}C NMR (400 MHz, $CDCl_3$): δ (ppm) 191.64, 144.32, 141.44, 128.29, 126.89, 126.59, 123.77, 122.79, 120.54, 120.17, 109.64, 109.10, 47.38, 39.48, 30.82, 28.64, 22.97, 14.00, 10.82. EM (EI) (M^+, $C_{21}H_{25}NO$): calcd, 307.19; found, 307.2.

*(E)-N′-((9-(2-ethylhexyl)-9H-carbazol-3-yl)methylene)-4-methylbenzenesulfonohydrazide (**3**).* Compound 2 (1.0 g, 6.5 mmol) and *p*-toluenesulfonyl hydrazide (0.75 g, 8.4 mmol) were dissolved in methanol (20 mL), and several drops of concentrated HCl (catalyst) solution were added in a dropwise manner. Then, the resulting solution was refluxed overnight. After cooling to room temperature, it was poured into water and extracted using dichloromethane. The combined organic phase was dried over anhydrous magnesium sulfate. The crude product was extracted from the solvent and purified by column chromatography using EA/hexane (composition ratio = 1:9). The yield of the product 3,

Table 2
Characteristics of P3HT/CBZ-C_{60} BHJ solar cells with different composition ratio.

	Composition ratio (P3HT/CBZ-C_{60})		
	1:0.5	1:0.7	1:1
V_{oc} (V)	0.60	0.61	0.64
J_{sc} (mA/cm^2)	1.61	2.07	2.32
FF (%)	29.6	31.1	32.6
PCE (%)	0.29	0.39	0.48

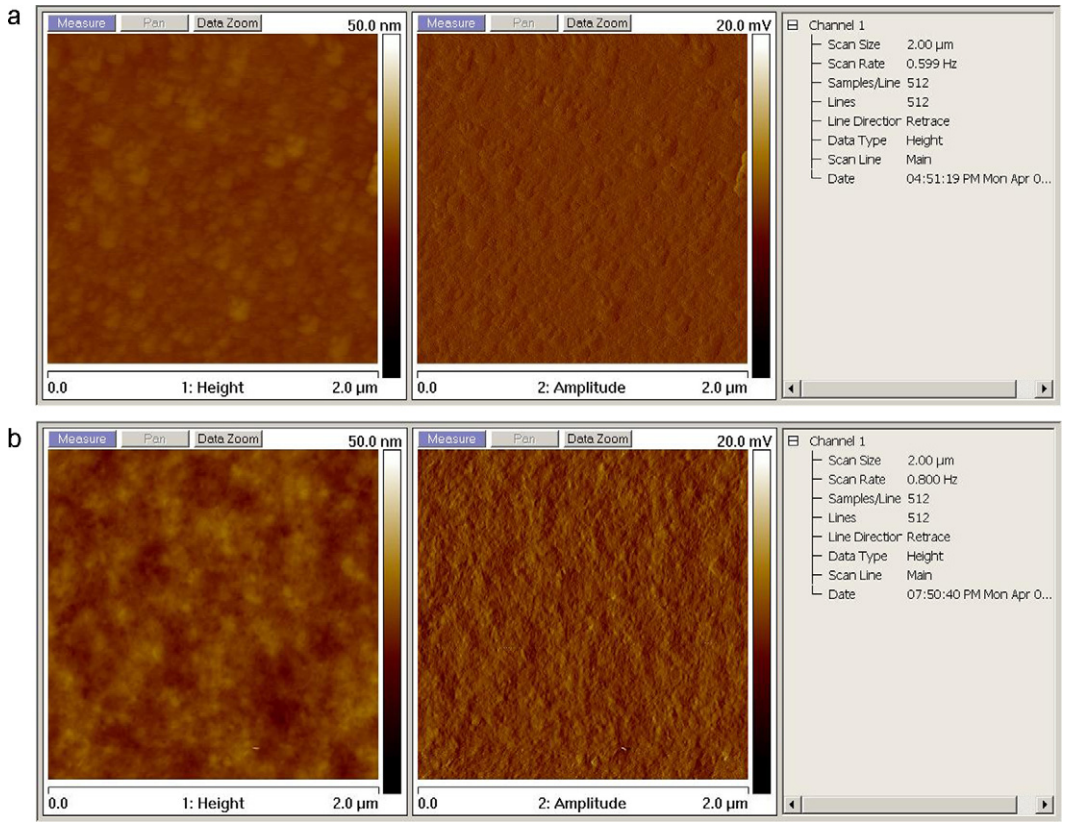

Fig. 6. AFM images of blend of P3HT with (a) PCBM (1:0.5), (b) CBZ-C_{60} (1:0.5) after annealing 10 min at 150 °C under atmosphere condition.

a yellow powder, was 89.3% (1.38 g). ^{1}H NMR (400 MHz, $CDCl_3$): δ (ppm) 8.23 (s, 1H), 8.06 (d, 1H), 7.94–7.89 (t, 3H), 7.72 (d, 2H), 7.46 (t, 1H), 7.37 (d, 1H), 7.30 (t, 3H), 4.12 (q, 2H), 2.37 (s, 3H), 2.02 (m, 1H), 1.35–1.30 (m, 8H), 0.89–0.82 (m, 6H). ^{13}C NMR (400 MHz, $CDCl_3$): δ (ppm) 150.311, 144.24, 142.33, 141.41, 135.60, 129.86, 129.76, 128.25, 128.15, 126.27, 125.11, 124.28, 122.92, 122.78, 120.70, 120.57, 119.63, 109.47, 109.31, 47.60, 39.50, 31.07, 28.90, 24.47, 23.19, 21.75, 14.22, 11.04. FAB-MS (M+1, $C_{28}H_{33}N_3O_2S$): calcd, 475.23; found, 476.

*CBZ-C_{60} (**4**).* Compound 3 (0.5 g, 1.05 mmol) was dissolved in dry pyridine (10 mL) under nitrogen. Then, sodium methoxide (0.12 g, 2.18 mmol) was added quickly under nitrogen, the resulting solution was stirred at room temperature for 20 min. C_{60} (0.6 g, 0.84 mmol) in dichlorobenzene was added in one portion. The resulting purple solution was heated to 80 °C and stirred for 48 h. Then, the solution was heated to reflux and stirred overnight. After cooling to room temperature, the solution was loaded into a silica column and pre-eluted with chlorobenzene and then with toluene. The fraction containing CBZ-C_{60} was collected and concentrated. The concentrated solution was poured into methanol. The crude product was collected by filtration and dried in a vacuum oven. Finally, the product was purified by successive extraction using the eluents methanol, hexane, and chloroform in a Soxhlet extractor. The product yield was 37.7% (0.4 g). ^{1}H NMR (400 MHz, $CDCl_3$): δ (ppm) 8.64 (s, 1H), 8.18 (d, 1H), 8.04 (d, 1H), 7.55–7.42 (m, 3H), 7.30 (m, 1H), 4.21 (m, 2H), 2.12 (m, 1H), 1.44–1.27 (m, 9H), 0.96 (t, 3H), 0.86 (t, 3H). ^{13}C NMR (400 MHz, $CDCl_3$): δ (ppm) 148.28, 146.23, 145.28, 144.88, 144.58, 143.30, 143.16, 142.30, 141.72, 123.43, 120.83, 109.39, 54.54, 39.72, 33.69, 31.22, 29.03, 24.64, 23.32, 14.32, 11.20. FTIR (KBr, cm^{-1}): 2953, 2862, 1460, 751, 725, 570, 525. FAB-MS (M+1, $C_{81}H_{25}N$): calcd, 1011.2; found, 1011.

3. Results and discussion

The new C_{60} derivative was soluble in common organic solvents such as dichloromethane, chloroform, toluene, chlorobenzene, and 1,2-dichlorobenzene. The solubility of C_{60} was improved by introducing an ethylhexyl-substituted carbazole group. We confirmed that CBZ-C_{60} was synthesized by ^{1}H NMR (Fig. 1). A characteristic two –CH_3 peaks were observed at 0.87 and 0.96 ppm and –CH_2– peak just adjacent to the carbazole nitrogen at 4.22 ppm.

The formation of CBZ-C_{60} was also confirmed by FTIR spectroscopy and UV–vis spectroscopy. Fig. 2a and b compared the FTIR spectra of C_{60}, 9-(2-ethylhexyl)-9H-carbazole and CBZ-C_{60}. 9-(2-Ethylhexyl)-9H-carbazole shows the characteristic absorption bands at 725 and 751 nm corresponding to the carbazole group [9], and at 2953 cm^{-1} (CH_3 stretching vibration), 2862 cm^{-1} (CH_2 stretching vibration), 1460 cm^{-1} (aromatic C=C stretching vibration). CBZ-C_{60} also shows the carbazole absorption at 725 and 751 cm^{-1} (doublet) as shown in Fig. 2a. C_{60} has characteristic absorption peaks in fingerprint region at 570 and 525 cm^{-1} associated with stretching vibrations of C_{60} molecule are observed in FTIR spectra of both C_{60} and CBZ-C_{60} at the same position as shown in Fig. 2b [10,11].

The UV–vis absorption spectra of C_{60}, 9-(2-ethylhexyl)-9H-carbazole, and CBZ-C_{60} in 1,2-dichlorobenzene solution are shown in Fig. 3. It is observed that two main absorption peaks at 285 and at 333 nm exist in the spectrum of C_{60} and the absorption edge exists over the entire visible spectrum. In the case of 9-(2-ethylhexyl)-9H-carbazole, strong absorption bands are observed at 300, 332 and 348 nm, and the onset absorption is observed at about 360 nm. These three absorption peaks of 9-(2-ethylhexyl)-9H-carbazole are also observed in the absorption of CBZ-C_{60}. Further, the absorption edge of CBZ-C_{60} extends farther into the longer

wavelength region than that of 2-ethylhexylcarbazole does. This is a characteristic property of C_{60} derivatives and indicates that the carbazole group is attached to the C_{60} cage.

The electrochemical properties of CBZ-C_{60} were studied by cyclic voltammetry by using 1,2-dichlorobenzene solution with $TBABF_4$ as the electrolyte (Fig. 4). The C_{60} derivatives exhibit several quasi-reversible one-electron reduction waves, which are attributed to the fullerene core. The onset reduction potential corresponding to the LUMO energy level of CBZ-C_{60} shifts to a value that is lower than the LUMO energy level of C_{60}. This happens because of the following reason: (1) the number of π-electrons in CBZ-C_{60} is higher than that in C_{60}. (2) Strain energy is released when a [6,6] methane substitute is introduced in C_{60} [12]. The LUMO energy level could be calculated from the onset reduction potential (E_{Red} (onset)) on the basis of the reference energy level of ferrocene (4.8 eV below the vacuum level, which is defined as zero [13,14]). LUMO = $-[(E_{Red}(onset) - E_{foc}) + 4.8]$ (eV), where E_{foc} is the potential of the external standard, the ferrocene/ferricenium ion (Foc/Foc^+) couple. The value of E_{foc}, which was determined under the same conditions as those for CBZ-C_{60}, is about 0.260 V versus $Ag/AgNO_3$. E_{Red} (onset) for CBZ-C_{60} is −0.856 V. Thus the LUMO energy level of CBZ-C_{60} is estimated to be −3.68 eV, which is much higher than that of C_{60} at the same condition (−3.78 eV). This is in agreement with the hypothesis that addition of an electron donating carbazole group to a C_{60} could improve its LUMO energy level. This LUMO energy level value of CBZ-C_{60} is quite similar to that of $PC_{61}BM$ (−3.70 eV) obtained at the same condition.

The performance of P3HT/CBZ-C_{60} BHJ devices were investigated by adopting the following configuration: ITO/PEDOT:PSS/P3HT:CBZ-C_{60}/LiF/Al. We used the ITO as the anode, PEDOT-PSS (thickness: 45 nm) as a buffer layer, P3HT/CBZ-C_{60} as the active layer, and LiF/Al as the compound cathode. We fabricated different devices with varied P3HT/CBZ-C_{60} composition ratios and with compound thin films annealed for different durations. We found that the optimized device was one with a P3HT/CBZ-C_{60} film that had a P3HT/CBZ-C_{60} composition ratio 1:1 and that was annealed at 150 °C for 10 min. Fig. 5 shows the *I–V* characteristics of devices with thin films that had a P3HT/CBZ-C_{60} composition ratio of 1:1 and that were annealed for different durations at 150 °C under AM 1.5 G illumination with an intensity of 100 mW/cm^2. The performance of these devices is summarized in Table 1. It has been found that increasing the annealing time from 5 to 10 min increased the power conversion efficiency (PCE) from 0.43% to 0.48%. Further, an increase in the short-circuit current was observed, which indicated that the mobility of the charge carriers inside the photoactive layer improved. We presume that this increase in the short-circuit current is due to an improvement in the crystallization of the polymer during the annealing process. However, no significant change in PCE was observed when the annealing time was varied gradually from 10 to 20 min. We also investigated the PCE of the devices with different ratios of the donor to the acceptor and found that the PCE of devices with thin films having P3HT/CBZ-C_{60} composition ratio of 1:1 was higher than those of devices with thin films having different composition ratios. The performance of the devices with dissimilar P3HT/CBZ-C_{60} composition ratios and annealed at 150 °C for 10 min are summarized in Table 2.

The maximum V_{oc} of the P3HT/CBZ-C_{60} devices was 0.64 V, and this V_{oc} was considerably higher than those of the reported P3HT/C_{60} double-layer device (0.34 V) [15] and comparable to those of the P3HT/PCBM BHJ devices (0.55–0.64 V) [4,16,17]. The highest short-circuit current density (J_{sc}) listed in Table 1, was 2.32 mA/cm^2 and the best PCE of the device based on CBZ-C_{60} was 0.48%.

Bulk hetero films of CBZ-C_{60} and P3HT were spin coated on glass substrates and were characterized by using AFM in order to study and compare their morphological features. Here we just measured the bulk hetero film of P3HT/CBZ-C_{60} with composition of 1:0.5 for example and compared the result with that of P3HT/PCBM which has the same blending ratio. The bulk hetero films were prepared as follows. P3HT and CBZ-C60 were dissolved in 1,2-dichlorobenzene at 1:0.5 wt ratio and stirred overnight. Then, the solution was spin coated on freshly rinsed glass plates after filtration and the glass plates were annealed at 150 °C for 10 min under atmosphere condition. The bulk hetero film containing P3HT and PCBM was prepared by using the same method.

Tapping-mode AFM measurements were performed on a scan size of 2 μm. As shown in Fig. 6, reference film containing P3HT and PCBM had a very flat surface (shown in Fig. 6a). However, the film containing P3HT and CBZ-C60 (shown in Fig. 6b) showed much rougher and aggregated surface morphology. The film with 1:0.5 blending ratio showed obvious chainlike features (brighter area) which are assigned to the domains of P3HT crystallites. The effective contact areas of P3HT and CBZ-C_{60} decreased rapidly resulting in much lower fill factor and short circuit current, which might be the main reason for the much lower PCE compared with the devices blending with P3HT and PCBM.

As discussed above, introduction of an electron donating group could modify the LUMO lever for modifying the V_{oc} and for better PCE [18]. However, bulky substituent in C_{60} could affect the morphology of the blending film and increase the distance between the balls and result in a decrease in the electron mobility. Furthermore, impurity, bi-adduct, was found in FAB-Mass spectrum, which would also affect power conversion efficiency of the solar cell devices based on CBZ-C_{60}.

Further optimization of BHJ solar cells and purer fullerene derivatives with both high V_{oc} and better electron mobility are under investigation.

4. Conclusions

A novel fullerene derivative CBZ-C_{60} was synthesized and characterized. The new C_{60} derivative showed good solubility in common organic solvents. Further, BHJ photovoltaic devices with the new C_{60} derivative as the electron acceptor and P3HT as the electron donor were fabricated; the configuration of these devices is as follows: ITO/PEDOT:PSS/active layer/LiF/Al. It was observed that the LUMO energy level of this derivative was significantly higher than that of fullerene C_{60} and is comparable with that of PCBM. The open circuit voltage of the devices based on the new derivative is comparable with those of devices based on PCBM. The highest PCE was 0.48% for a device with a P3HT/CBZ-C_{60} film that has a composition ratio of 1:1 and that was annealed at 150 °C for 10 min.

Acknowledgments

This research was financially supported by the Ministry of Knowledge Economy (MKE) under the New & Renewable Energy Program through a KETEP grant (No. 20103020010050), and a grant from the cooperative R&D Program (B551179-08-03-00) funded by the Korea Research Council Industrial Science and Technology, Republic of Korea, and the Research Fund Program of Research Institute for Basic Sciences, Pusan National University, Korea, 2011, Project No. RIBS-PNU-2011-302.

References

[1] G. Yu, J. Gao, J.C. Hummelen, F. Wudl, A.J. Heeger, Science 270 (1995) 1789–1791.
[2] M. Svensson, F. Zhang, S.C. Veenstra, W.J.H. Verhees, J.C. Hummelen, J.M. Kroon, O. Inganas, M.R. Andersson, Adv. Mater. 15 (2003) 988–991.
[3] S.E. Shaheen, C.J. Brabec, N.S. Sariciftci, F. Padinger, T. Fromherz, J.C. Hummelen, Appl. Phys. Lett. 78 (2001) 841–843.

[4] W. Ma, C. Yang, X. Gong, K. Lee, A.J. Heeger, Adv. Funct. Mater. 15 (2005) 1617–1622.
[5] J. Peet, J.Y. Kim, N.E. Coates, W.L. Ma, D. Moses, A.J. Heeger, G.C. Bazan, Nat. Mater. 6 (2007) 497–500.
[6] H.L. Yip, S.K. hau, N.S. Beak, A.K.-Y. Jen, Appl. Phys. Lett. 92 (2008) 193313–193321.
[7] N. Martin, L. Sancheza, D.M. Guldi, Chem. Commun. 2 (2000) 113–114.
[8] F.B. Kooistra, J. Knol, F. Kastenberg, L.M. Popescu, W.J.H. Verhees, J.M. Kroon, J.C. Hummelen, Org. Lett. 9 (4) (2007) 551–554.
[9] M. Wainwright, J.J. Griffths, T. Guthrie, A.P. Gates, D.E. Murry, J. Appl. Polym. Sci. 44 (1992) 1179–1186.
[10] K. Nakamoto, M.A. Mckinney, J. Chem. Educ. 77 (2000) 775–779.
[11] C.I. Frum, R. Engleman Jr., H.G. Hedderich, P.F. Bernath, L.D. Lamb, D.R. Huffman, Chem. Phy. Lett. 176 (1991) 504–508.
[12] Y. Zhang, H.-L. Yip, O. Acton, K.H. Steven, K.-Y.J. Alex, Chem. Mater. 21 (2009) 2598–2600.
[13] J.L. Bredas, R. Silbey, D.S. Boudreaux, R.R. Chance, J. Am. Chem. Soc. 105 (1983) 6555–6559.
[14] Y.Z. Lee, X.W. Chen, S.A. Chen, P.K. Wei, W.S. Fann, J. Am. Chem. Soc. 123 (2001) 2296–2307.
[15] L.R. Gearba, C.-Y. Nam, R. Pindak, C.T. Black, Appl. Phys. Lett. 95 (2009), 173307-1–173307-3.
[16] F. Padinger, R.S. Rittberger, N.S. Sariciftci, Adv. Funct. Mater. 13 (2003) 85–88.
[17] M.D. Irwin, J. Liu, B.J. Leever, J.D. Servaites, M.C. Hersam, M.F. Durstock, T.J. Marks, Langmuir 26 (2010) 2584–2591.
[18] D. Mi, J.-H. Kim, F. Xu, S.-H. Lee, S.C. Yoon, W.S. Shin, S.-J. Moon, C. Lee, D.-H. Hwang, Sol. Energy Mater. Sol. Cells 95 (2011) 1182–1187.